available at www.sciencedirect.com
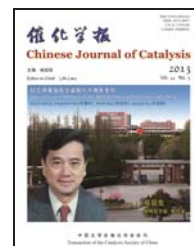
ScienceDirect

journal homepage: www.elsevier.com/locate/chnjc

Article (Special Issue in Memory of the 80th Birthday of Professor Jingfa Deng)

# Carbon-coated mesoporous silica functionalized with sulfonic acid groups and its application to acetalization

FANG Lin, ZHANG Kun #, CHEN Lu, WU Peng *

*Shanghai Key Laboratory of Green Chemistry and Chemical Processes, Department of Chemistry, East China Normal University, Shanghai 200062, China*

ARTICLE INFO

ABSTRACT

The inner surface of mesoporous silica SBA-15 was coated by a homogeneous polycyclic carbon layer through controlled carbonization of furfuryl alcohol. The composite was subsequently functionalized with sulfonic acid ($-SO_3H$) groups to form a strong solid acid material, with a tunable acid site density in the range of 0.38–0.84 mmol/g by varying the thickness of the carbon layer. Structural analysis and reaction data revealed that the solid acid catalyst exhibited high reactivity towards the acetalization of aldehydes or ketones with alcohols because of the uniform carbon coating of the mesopores, high acid site density, and its mechanical stability.

## 1. Introduction

Solid acid catalysts have been widely applied in petroleum refining and fine chemical production processes because of a number of advantages, including their convenient reuse, long-term activities, and low environmental pollution. Solid acids such as metal oxides [1,2], heteropoly acids [3,4], sulfonic acid group-functionalized materials [5,6], and acidic ion exchange resins [7,8] can effectively replace homogeneous acids, including sulfuric acid, fatty acid salts [9], and organic sulfonic acid [10], in various acid-catalyzed reactions, such as the Beckmann rearrangement [11,12], alkylation [13], esterification and hydrolysis [5,6], acylation [14], etherification [15], addition reaction of the epoxides and olefin adducts as well as the dehydration of the alcohols [16,17], condensation [18,19], and hydrogenation reforming [20].

Recently, heterogeneous acids containing sulfonic acid groups, including ionic liquids [21], organic-inorganic hybrid porous materials [22,23] and sugar derived carbon catalysts [24], have been intensively investigated, because of their abundant acid content and effective activities. Xing et al. [25] reported a sulfonated mesoporous carbon material with a classical CMK-3 type mesostructure, applying SBA-15 as a hard template filled with sucrose, which was subsequently carbonized incompletely to a polycyclic aromatic carbon. The aromatic system is rich in benzene rings that can be controllably grafted by sulfonic acid groups, leading to a novel mesoporous solid acid CMK-3-$SO_3H$. Compared with the sulfonated sugar carbon acid (2 m²/g) from Nakajima et al. [26], it possesses a large specific surface area of nearly 1000 m²/g and 1.0 mmol/g Brönsted acid sites and shows an excellent catalytic activity towards the liquid phase Beckmann rearrangement. However, the carbon framework of CMK-3-$SO_3H$ is fragile in practical applications, especially during sulfonation because the frame-

work tends to collapse with over-carbonation by the sulfuric acid. Accordingly, Fang et al. [6] further simplified the synthetic procedure to make a sulfonic functionalized carbon-silicon composite, which exhibited high stability and chemical reactivity for esterification and transesterification in biodiesel synthesis after several recycles because of pillaring of silica in the composites. Increasing the carbon loading in a carbon-silica composite can provide more benzene rings for functionalization by sulfonic acid groups but, nevertheless, the bulk aromatic carbon is randomly distributed in the pores or on the channel entrance of SBA-15, which significantly limits the diffusion of large molecules in confined nanospaces.

As is well known, acetalization is generally used to protect the carbonyl group of aldehydes and ketones and, moreover, the acetal is the main raw enantiomeric compound used in the production of anabolic steroids, pharmaceuticals, paint, and perfumes, which often involves large molecules. The reaction is usually catalyzed by homogeneous acids to obtain high yield and selectivity [27]. Although heteropoly acids [21] and ionic liquid catalysts give high yields, greater than 90%, long reaction times are necessary because of their low acidity [28]. Sulfonated nano silica fibers with high acidity are a good candidate; however, their low surface area and small pore volume dramatically reduce the reaction rate [29].

Here, based on a method to synthesize CMK-5 with furfuryl alcohol [30], we prepared a carbon-silica composite with an aromatic carbon layer decoration on the pore walls of mesoporous silica, using furfuryl alcohol as the carbon source. A SBA-15 silica support was pretreated by incorporation of $Al^{3+}$, which modifies the silica wall with a dispersion of acid sites that then catalyze the carbonization of furfuryl alcohol. The resultant Al-SBA-15 was loaded by furfuryl alcohol, which was then converted to a polycyclic benzene ring carbon coating on the silica wall under a sequence of vacuum extraction and appropriate thermal treatment. Finally, the composite was sulfonated to obtain a mesoporous carbon-silica solid acid, reserving the hollow channels to retain a large surface area and accessible acid sites. This material exhibits a high catalytic reactivity towards the acetalization of aldehydes or ketones with alcohol and is stable during recycled usage.

## 2. Experimental

### 2.1. Material preparation

Mesoporous SBA-15 was synthesized by the conventional approach using poly(ethyleneoxide)-poly(propyleneoxide)-poly(ethyl-eneoxide) (P123, $M_W \approx 5800$, Sigma-Aldrich) and tetraethyl orthosilicate (TEOS, Sigma-Aldrich) in acidic media [6]. One gram of calcined SBA-15 was treated with $Al^{3+}$ in a 25 ml anhydrous alcohol (China National Medicines Corporation Ltd.) solution containing 0.12 g $AlCl_3$ (China National Medicines Corporation Ltd.) at a Si/Al molar ratio of 20:1 [31]. After stirring at room temperature for 14 h, the Al-incorporated SBA-15 was filtered, washed three times with anhydrous alcohol, and then dried at 80 °C, followed by calcination at 550 °C in air for 6 h. The resultant white solid product was named Al-SBA-15 and

had a Si/Al molar ratio of 19.2, determined by elemental analysis.

Subsequently, the aluminosilicate was filled with furfuryl alcohol (>98.0%, China National Medicines Corporation Ltd.) at room temperature using an incipient wetness method. The amount of furfuryl alcohol was varied over a furfuryl alcohol/Al-SBA-15 mass ratio of 0.5-5, respectively. The filled aluminosilicate was heated at 80 °C for 1 h to polymerize the furfuryl alcohol and then exposed to extraction under vacuum at the same temperature for 1 h to remove the excess alcohol. Finally, calcination was continued under $N_2$ at 550 °C for 6 h to obtain the carbon-silica composite, which was named SC-$x$ ($x$ = mass change due to the carbon compound according to the thermogravimetric analysis profile, e.g. $x$ = 15 indicates a 15% mass change). The SC-$x$ was mildly sulfonated at 80 °C in an atmosphere of fuming sulfuric acid (50%$SO_3$/$H_2SO_4$, China National Medicines Corporation Ltd.), with a ratio of solid/liquid = 1:20 g/ml for 12 h. To extract the physically adsorbed –$SO_3H$ group, the solid acid was finally washed with water at >80 °C until no white precipitate could be detected in the filtrate with $BaCl_2$ (≥98.0%, China National Medicines Corporation Ltd.), and dried to obtain the surfonated carbon-silica composite SC-$x$-$SO_3H$.

The SC-$x$ and SC-$x$-$SO_3H$ were liberated from the silica template by treatment with 15% HF (≥ 40%, China National Medicines Corporation Ltd.) solution at a ratio of solid/liquid = 1:20 g/ml under stirring at room temperature overnight, followed by washing with ionized water and drying to obtain CMK-5 type materials, named C-$x$ and C-$x$-$SO_3H$, respectively.

Sulfonated carbon-silica composites using sucrose were prepared according to the method reported by Fang et al. [6].

### 2.2. Characterization

Powder X-ray diffraction (XRD) patterns were collected on a Bruker D8 ADVANCE instrument using Cu-$K_\alpha$ radiation ($\lambda$ = 0.15406 nm). $N_2$ adsorption isotherms were measured at –196 °C on a Quantachrome Autosorb-3B instrument after activating the sample at 120 °C under vacuum for 6 h. Scanning electron microscopy (SEM) images were obtained with a Hitachi S-4800 microscope. Fourier transform infrared (FT-IR) spectra were recorded on a Nicolet Fourier transform infrared spectrometer (NEXUS 670) using KBr. The spectra of pyridine adsorption were measured by first treating the sample wafers at 150 °C under vacuum for 5 h and then exposing them to pyridine vapor at 110 °C for 0.5 h. Desorption of pyridine was carried out at 150 °C. Thermogravimetric (TG) analysis curves were obtained on a Mettler analyzer (TGA/SDTA 851e/5FL1100). The acid density was quantified by acid-base titration whereby 0.15±0.01 g solid acid was ion-exchanged in 60 ml saturated NaCl solution at room temperature for 12 h and then filtered, followed by titration of the filtrate against NaOH solution, which had been standardized by potassium acid phthalate.

### 2.3. Catalytic test

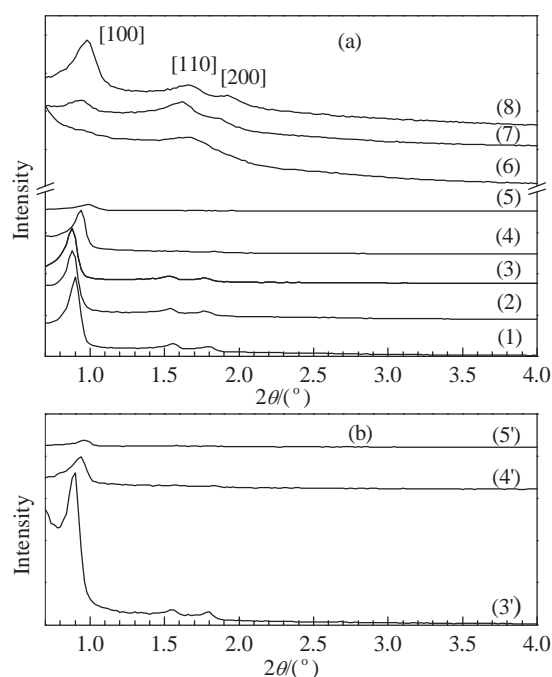The aldehyde or ketone 0.04 mol, alcohol 0.048 mol (cyclo-

hexanone, cyclopentanone, iso-valeraldehyde, iso-butyraldehyde, 3-pentanone, ethylene glycol, and 1,4-butanediol were from China National Medicines Corporation Ltd.; benzaldehyde, 3-Methyl butanal, and diphenyl ketone were from TCI supplier), catalysts (40 mg), and 5 ml of cyclohexane (> 99.5%, China National Medicines Corporation Ltd.) were placed in a 100 ml three-necked flask and mixed. The flask was connected to a condenser and a trap to the remove the water product by azeotropic distillation. After reacting at 90 °C under reflux for 1 h, the products were analyzed on an Agilent 6890/5973N gas chromatography-mass spectrometer (GC-MS) and quantified on a Shimadzu 14B FID GC with a DB-WAX capillary column ($\phi$ 0.25 mm × 30 m) using eicosane as an internal standard.

## 3. Results and discussion

### 3.1. Structure and chemical properties of catalyst

It has been reported that sulfonic group can be induced to a greater extent by increasing the loading of polycyclic benzene rings in SBA-15 [6]. Therefore, the relevance of sulfonate group content and carbon content in the SC-$x$-SO$_3$H materials was investigated (Table 1) by studying the effect of extracting excess furfuryl alcohol under vacuum. The composite after extraction could be loaded by the carbon compound to a maximum of $x$ = 65% and when $x$ = 51%, the acid content was the highest, at 0.84 mmol/g. By comparison, samples prepared without extraction were limited to a carbon loading of 52%, leading to a maximum acid content of 0.71 mmol/g, which was the same as that of a composite with vacuum extraction loaded with 44 wt% carbon. As displayed in the XRD patterns (Fig. 1(a), (8)), the excess introduction of furfuryl alcohol resulted in pore blockage in SBA-15, resulting in a CMK-3-type material with solid nanotubes after removing the silica template.

After the sequence of post-incorporation of Al$^{3+}$ and furfuryl alcohol loading, the SC-$x$ materials retained a uniform 2D hexagonal mesopore array, as shown in the XRD patterns in Fig. 1(a). The peaks assigned to the [100], [110], and [200] diffractions of the 2D hexagonal structure (*p6mm*) of SBA-15 became gradually weaker in intensity with increasing carbon loading in the mesopores. This can be attributed to the diffraction inter-

**Table 1**
Comparison of the CHO loading and –SO$_3$H acid density in SC-$x$-SO$_3$H with and without evacuation at 80 °C.

| Furfuryl alcohol/ Al-SBA-15 mass ratio | CHO* (wt%) | | H$^+$ (mmol/g) | |
|---|---|---|---|---|
| | Evacuation | Without evacuation | Evacuation | Without evacuation |
| 0.5 | 15 | 26 | 0.38 | 0.41 |
| 0.75 | — | 34 | — | 0.60 |
| 1 | 26 | 40 | 0.42 | 0.62 |
| 1.5 | 34 | 48 | 0.56 | 0.60 |
| 2 | 41 | 52 | 0.62 | 0.71 |
| 2.5 | 44 | — | 0.71 | — |
| 3 | 51 | — | 0.84 | — |
| 4 | 61 | — | 0.65 | — |
| 5 | 65 | — | 0.48 | — |

* Mass change by TG analysis in the 200–800 °C.



**Fig. 1.** Low-angle XRD patterns of samples before (a) and after (b) sulfonation. (1) SBA-15; (2) Al-SBA-15; (3) SC-26; (4) SC-34; (5) SC-44; (6) C-34; (7) C-44; (8) C-52; (3') SC-26-SO$_3$H; (4') SC-34-SO$_3$H; (5') SC-44-SO$_3$H.

ference from the carbon filling rather than a structural collapse (Fig. 1(a)). Moreover, the [100] peak broadening indicates a regional structure distortion of SBA-15 caused by excess carbon loading.

After the removal of silica, C-$x$ materials consisting of polycyclic benzene rings present a typical CMK-5-type mesoporous structure characteristic wherein diffraction peak [110] is more intensive than peak [100] [30]. This reveals that after the 550 °C calcination, furfuryl alcohol was converted into hollow nanotubes of the polycyclic benzene rings coating the silica wall, where the Al$^{3+}$ was incorporated and catalyzed the polymerization. Greater carbon filling intensified peak [100], indicating that the wall of the nanotube was thickened and even transformed to the solid stick-like mesostructure of the CMK-3-type (Fig. 1(a)). The diffraction peaks were maintained after sulfonation (Fig. 1(b)), implying that the acid-inert silica support could protect the ordered structure of SC-$x$-SO$_3$H.

The N$_2$ adsorption-desorption isotherms and pore size distribution of SBA-15 and SC-$x$-SO$_3$H materials are demonstrated in Fig. 2(a) and (b), respectively, and their textural properties are listed in Table 2. With increasing carbon loading, the specific surface area of the composites decreased from 761 cm$^3$/g in the SBA-15 support to 472 cm$^3$/g in the SC-34-SO$_3$H, and the pore size was simultaneously reduced from 8.1 to 3.6 nm. However, SC-$x$-SO$_3$H (when $x$ < 44) still had the classic type IV isotherm, indicating the presence of an ordered mesoporous structure (Table 2, Fig. 2(a) and 2(b)). The adsorption-desorption isotherms of SC-34-SO$_3$H began to disconnect, attributed to the typical structural features of organic mesoporous polymers that indicate a uniform coating of polycyclic benzene rings on the silica mesopore walls. At the same time,
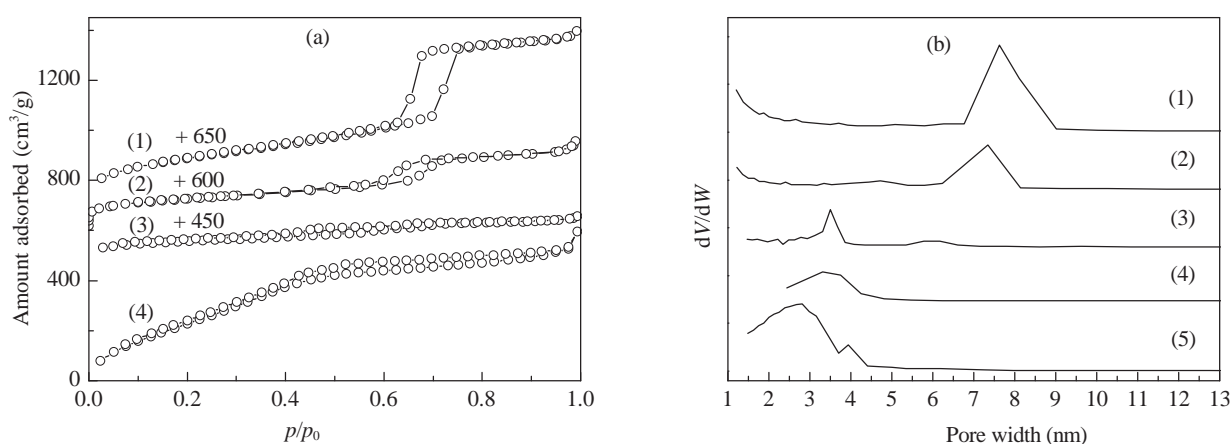
**Fig. 2.** (a) N$_2$ adsorption-desorption of SBA-15 (1), SC-15-SO$_3$H (2), SC-34-SO$_3$H (3), and C-44 (4), and (b) BJH pore diameter distribution of SBA-15 (1), SC-15-SO$_3$H (2), SC-34-SO$_3$H (3), SC-44-SO$_3$H (4), and C-44 (5).

the relative pressure of the hysteresis loop $p/p_0 = 0.65$–$0.70$ shifted to $p/p_0 = 0.5$, showing a reduced pore volume because of the increasing carbon coating layer. Furthermore, the layered benzene ring carbon generated 27% micropores in the total volume (Table 2), thus the hysteresis loop indicated a two-step desorption phenomenon (Fig. 2(a)). When the carbon loading was $x > 50$, the isotherm was converted to type I and the specific surface area of SC-51-SO$_3$H was reduced to 318 cm$^3$/g, with the micropore volume increasing to 48% of the total, which is higher than that of the 45%C/CS-SO$_3$H (272 cm$^3$/g) reported previously using sucrose as a carbon source [6], indicating the presence of a mesoporous structure.

After removing the silica template, C-34 and C-44 appeared to have a type IV adsorption isotherm at $p/p_0 = 0.35$ and a steep capillary condensation, indicating a regular mesoporous structure. In addition, the existence of an unclosed hysteresis loop in the adsorption-desorption isotherms showed that the material consists of an organic framework as the mesoporous FDU-15, which is a polymerized phenolic resin [23]. Moreover, the C-$x$ samples have a superposed double-pore size distribution, similar to that of CMK-5, showing that the hollow carbon nanotubes formed in C-$x$ have a typical hexagonal close-packed structure (Fig. 2(a), (4); Fig. 2(b), (5)). The double-pore size distribution on the right of the figure is attributed to the diameter of the poly-benzene ring carbon nanotube coating on the silica wall, while on the left, the broader distribution is caused

by the tube gap, which depends on the thickness of the SBA-15 pore wall as well as wall-attached species such as Al [30]. The thickness of the carbon nanotube wall was increased with greater furfuryl alcohol loading (Table 2, C-34 and C-44), and the presence of hollow tubes greatly promotes the transport and diffusion of macromolecules within the pores.

The SEM images provide further evidence that the C-44-SO$_3$H material has a similar mesoporous structure to that of CMK-5. It has a 2D hexagonally close-packed tube arrangement, with a wall thickness of approximately 2 nm and an irregular tube gap of approximately 4 nm (Fig. 3). This structure remains after sulfonation, further indicating the high stability of its mechanical, physical, and chemical properties.

Incorporated sulfonic groups can be determined by FT-IR spectra, as shown in Fig. 4(a). A broad absorption peak in the region 1000–1300 cm$^{-1}$ observed on SC-34-SO$_3$H sample is attributed to the Si–O stretching vibration, while a sharp peak appears at 1032 cm$^{-1}$ after removing the silica, assigned to the symmetric S=O stretching, indicating that the –SO$_3$H groups

**Table 2**

Textural properties of SC-$x$-SO$_3$H and C-$x$ samples.

| Sample | $A_{BET}$/ (m$^2$/g) | Pore volume (cm$^3$/g) | $V_{micro}$ [a]/% | $d$ [b]/nm |
|---|---|---|---|---|
| SBA-15 | 761 | 1.17 | 6 | 8.1 |
| SC-34-SO$_3$H | 472 | 0.37 | 27 | 3.6 |
| SC-44-SO$_3$H | 442 | 0.27 | 41 | 3.4 |
| SC-51-SO$_3$H | 318 | 0.20 | 48 | <2.0 |
| C-34 | 1420 | 1.15 | — | 4.2[c] (1.9[d]) |
| C-44 | 1112 | 0.89 | — | 3.9 (2.1) |

[a] Pore volume from $t$-plots, $V_{micro} = 100\% \times V_{micro}/(V_{micro} + V_{meso})$.

[b] BJH method.

[c] Nanotube width.

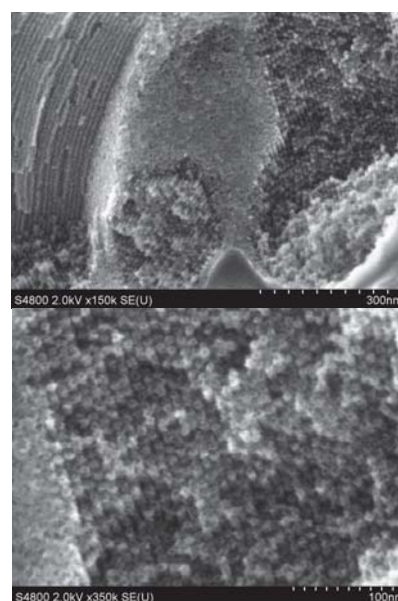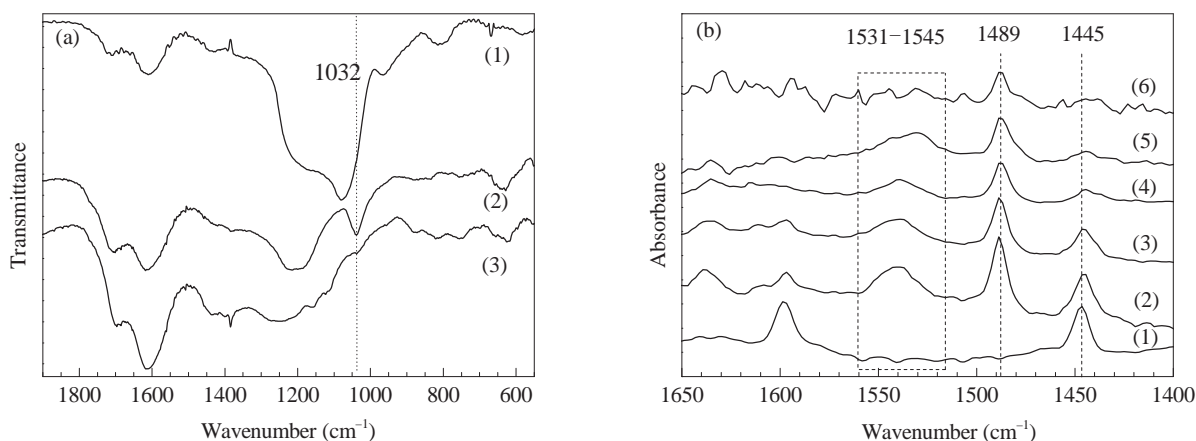[d] Thickness of nanotube = $(d_{SBA-15} - d_{nanotube})/2$.



**Fig. 3.** SEM images of C-44-SO$_3$H samples.

**Fig. 4.** (a) FT-IR spectra of SC-34-SO₃H (1), C-34-SO₃H (2), and C-34 (3), and (b) FT-IR spectra of adsorbed pyridine after desorption at 150 °C for SBA-15 (1), SC-15-SO₃H (2), SC-26-SO₃H (3), SC-34-SO₃H (4), SC-44-SO₃H (5), and SC-51-SO₃H (6).

have been successfully grafted onto the polycyclic benzene ring. Compared with C-34, a significant absorption band can be observed at about 1210 cm⁻¹ for C-34-SO₃H, which is attributed to the −COOH group in the mode of C=O stretching vibration, revealing that sulfonation also catalyzed the conversion of organic carbon compounds into carboxylic acid groups [24,26].

FT-IR spectrum of adsorbed pyridine was applied to verify the type and density of acid sites [31]. Sulfonated samples were dehydrated at 150 °C under vacuum, then cooled to 110 °C, adsorbing pyridine, finally followed by desorption at 150 °C to avoid physical adsorption [6]. Fig. 4(b) shows the FT-IR spectra of SC-$x$-SO₃H materials after pyridine adsorption with a series of absorption bands in the range 1531–1545, 1489, and 1445 cm⁻¹ caused by pyridine ring stretching. These correspond to the combination of pyridine with the Brönst acid sites, the Brönst acid sites and/or Lewis acid sites, and the Lewis acid sites and/or Si-OH, respectively. Increasing the furfuryl alcohol loading did not affect the peak intensity in the range of 1531–1545 cm⁻¹. When the loading of alcohol was further increased, the numbers of acid sites were sharply reduced for the SC-51-SO₃H sample. Two reasons are proposed: one is that the hydrogen bonding generated by increasing sulfonic acid groups stops the combination of pyridine and B acid sites; the other is that the accessibility of acid sites was blocked by thickening of the carbon layer (pore size less than 2.0 nm, Table 2).

### 3.2. Catalytic reaction

Because acid content and specific surface area are the two main factors that influence activity, the solid acid catalysts prepared with furfuryl alcohol and sucrose as carbon source, respectively, were compared for the acetalization of cyclopentanone and ethylene glycol (Fig. 5). For both materials, when the carbon precursor loading was less than 35%, the amount of sulfonic acid increased with carbon loading. The maximum acid value for the composite synthesized with sucrose was 0.70 mmol/g when $x$ = 35, while for the furfuryl alcohol composite, it was up to 0.84 mmol/g at $x$ = 50 carbon loading. Note that the latter, with 50% carbon, had nearly 100 m²/g higher surface

area than the former, thus the solid acid synthesized using furfuryl alcohol catalytically yielded a maximum of 82 mol% acetal compared with 63 mol% by sucrose composites. According to a previous report [6], the composite using sucrose as carbon precursor easily caused SBA-15 pore blockage with increasing carbon, which sharply decreased the surface area and pore volume, and its maximum acid value was reached at $x$ = 35. In contrast, the carbon layer derived from furfuryl alcohol was a uniform coating on the silica wall of SBA-15, and this improved the substitution of acid groups, leading to a higher acid intensity. Moreover, the stable mesostructure with hollow nanotubes can provide a larger reaction space that not only increases the accessible acid sites but also enhances the transport and diffu-
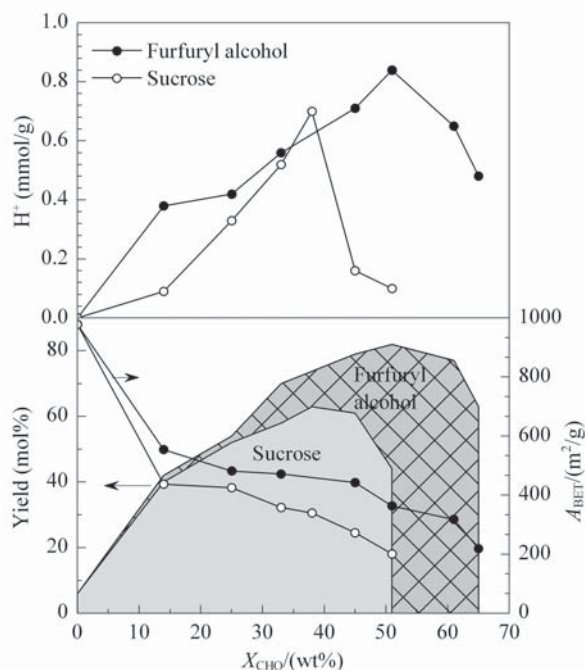


**Fig. 5.** Acetalization of cyclopentanone on the SC-$x$-SO₃H and $x$%C/CS-SO₃H, respectively. Reaction conditions: cyclopentanone 40 mmol, ethylene glycol 48 mmol, cyclohexane 5 ml, catalyst 40 mg, 90 °C, 1 h.

sion of the substrate and/or product.

Because of the considerable active amount of acid and large reaction space, SC-34-SO₃H was tested to further investigate the catalytic activity of the solid acid SC-*x*-SO₃H on acetalization of large molecules. The acetalization of iso-valeraldehyde, iso-butyraldehyde, benzaldehyde, and cyclohexanone with ethylene glycol all showed >90% yield, indicating the high catalytic activity of SC-34-SO₃H (Table 3, entries 1, 3, 5 and 7), while for 1,4-butanediol, the yield is slightly reduced by about 5% (Table 3, entries 2, 4, 6, and 8). In addition, when using 3-pentanone or benzophenone as substrates, the yield continued to decrease because of pore size restriction and also the steric effect of the large molecules, which have branched chains with a C=O functional group in the middle. Clearly, the presence of such hidden or diffusion-limited sulfonic acid groups resulted in a reduced yield of the product (Table 3, entries 9–12). The reaction of benzaldehyde and ethylene glycol could yield 91%, indicating that SC-34-SO₃H has a high reactivity towards molecules as large as benzaldehyde (Table 3, entry 5), while replacing this with benzophenone yielded 56% acetal after 5 h (Table 3, entry 11). Compared with benzaldehyde, benzophenone has twice the rigid size, thus only half the amount can be held in the same reaction space within the catalyst, probably leading to nearly half the yield. Similarly, the reaction of benzophenone and 1,4-butanediol yielded 25%, which is exactly half of the

yield from the reaction using ethylene glycol as the alcohol (Table 3, entries 11 and 12) because of the difference between the alcohol sizes. This further supports the existence of considerable amounts of acid sites and a facile accessibility, which enable superior reactivity towards acetalization.
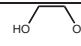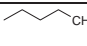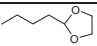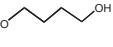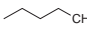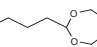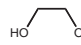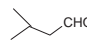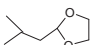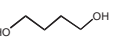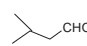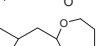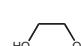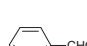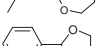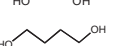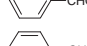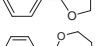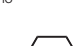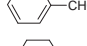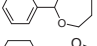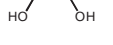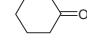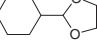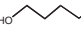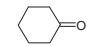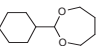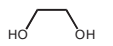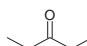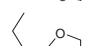
After the reaction of cyclohexanone and ethylene glycol, SC-34-SO₃H solid acid catalyst was recovered by filtration, washed thoroughly with cyclohexane and dried. The catalyst was then tested for reuse six times, finally obtaining a yield reduction of about 5%. Note that the poly-benzene ring layer formed under the $Al^{3+}$ catalyzed thermal polymerization and vacuum extraction was firmly attached onto the silica wall, and the composite demonstrated a high stability during reuse.

## 4. Conclusions

Furfuryl alcohol loaded SBA-15 was thermally polymerized at 550 °C into the polycyclic benzene ring carbon layer coated on the silica wall as regular hollow carbon nanotubes. After sulfonation, a functionalized carbon-silica solid acid was obtained with variable sulfonic acid sites. The catalyst shows excellent activity towards the acid-catalyzed acetalization of bulky aldehyde or ketone molecules with alcohols and is expected to be widel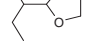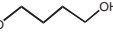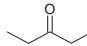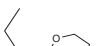y applicable because of its easy preparation and post-handling, compared with composites using sucrose as a carbon precursor.

**Table 3**
Acetalization of various aldehydes or ketones on the SC-34-SO₃H catalyst.

| Entry | Alcohol | Aldehyde or ketone | Product | Yield (mol%) |
|---|---|---|---|---|
| 1 | | | | 95 |
| 2 | | | | 88 |
| 3 | | | | 92 |
| 4 | | | | 86 |
| 5 | | | | 91 |
| 6 | | | | 86 |
| 7 | | | | 98 |
| 8 | | | | 92 |
| 9 | | | | 81 |
| 10 | | | | 26 |
| 11 | | | | 56* |
| 12 | | | | 25 |

Reaction conditions: aldehyde or ketone 40 mmol, alcohol 48 mmol, cyclohexane 5 ml, catalyst 40 mg, 90 °C, 1 h (* 5 h).

## References

[1] Pillai S K, Gheevarghese O, Sugunan S. *Appl Catal A*, 2009, 353: 130
[2] Katada N, Iseki Y, Shichi A, Fujita N, Ishino I, Osaki K, Torikai T, Niwa M. *Appl Catal A*, 2008, 349: 55
[3] Shimizu K, Niimi K, Satsuma A. *Appl Catal A*, 2008, 349: 1
[4] Atia H, Armbruster U, Martin A. *J Catal*, 2008, 258: 71
[5] Fang L, Xing R, Wu H H, Li X H, Liu Y M, Wu P. *Sci China Chem*, 2010, 53: 1481
[6] Fang L, Zhang K, Li X H, Wu H H, Wu P. *Chin J Catal* (方林, 张坤, 李晓红, 吴海虹, 吴鹏. 催化学报), 2012, 33: 114
[7] Harmer M A, Sun Q. *Appl Catal A*, 2001, 221: 45
[8] Saha M S, Nishiki Y, Furuta T, Denggerile A, Ohsaka T. *Tetrahedron Lett*, 2003, 44: 5535
[9] Serio M D, Tesser R, Dimiccoli M, Cammarota F, Nastasi M, Santacesaria E. *J Mol Catal A*, 2005, 239: 111
[10] Liu K S. *J Am Oil Chem Soc*, 1994, 71: 1179
[11] Wang X G, Chen C C, Chen S Y, Mou Y, Cheng S. *Appl Catal A*, 2005, 281: 47
[12] Ratnama K J, Reddy R S, Sekhar N S, Kantama M L, Deshpande A, Figueras F. *Appl Catal A*, 2008, 348: 26
[13] Zareyee D, Karimi B. *Tetrahedron Lett*, 2007, 48: 1277
[14] Das B, Kanth B S, Reddy K R, Kumar A S. *J Heterocyclic Chem*, 2008, 45: 1499
[15] Barrault J, Jerome F. *Eur J Lipid Sci Technol*, 2008, 110: 825
[16] Saikia L, Satyarthi J K, Srinivas D, Ratnasamy P. *J Catal*, 2007, 252: 148
[17] Dias A S, Pillinger M, Valente A A. *J Catal*, 2005, 229: 414
[18] Shimizu K, Hayashi E, Hatamachi T, Kodama T, Higuchi T, Satsuma A, Kitayama Y. *J Catal*, 2005, 231: 131
[19] Landge S M, Berryman M, Török B. *Tetrahedron Lett*, 2008, 49: 4505
[20] Balaraju M, Rekha V, Prasad P S S, Devi B L A P, Prasad R B N,

**Graphical Abstract**

*Chin. J. Catal.*, 2013, 34: 932–941      doi: 10.1016/S1872-2067(12)60591-9

**Carbon-coated mesoporous silica functionalized with sulfonic acid groups and its application to acetalization**

FANG Lin, ZHANG Kun*, CHEN Lu, WU Peng*
*East China Normal University*

Polycyclic carbon-coated SBA-15 serves as a stable solid acid catalyst after sulfonation, and is efficient during acetalization of aldehydes/ketones with alcohol because of its high surface area and abundant Brönsted acid sites.
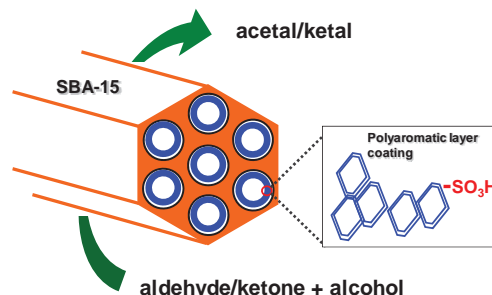
Lingaiah N. *Appl Catal A*, 2009, 354: 82

[21] Li D M, Shi F, Peng J J, Guo Sh, Deng Y Q. *J Org Chem*, 2004, 69: 3582

[22] Shimizu K, Hayashi E, Hatamachi T, Kodama T, Higuchi T, Satsuma A, Kitayama Y. *J Catal*, 2005, 231: 131

[23] Xing R, Liu N, Liu Y M, Wu H H, Jiang Y W, Chen L, He M Y, Wu P. *Adv Funct Mater*, 2007, 17: 2455

[24] Toda M, Takagaki A, Okamura M, Kondo J N, Hayashi S, Domen K, Hara M. *Nature*, 2005, 438: 178

[25] Xing R, Liu Y M, Wang Y, Chen L, Wu H H, Jiang Y W, He M Y, Wu P. *Microporous Mesoporous Mater*, 2007, 105: 41

[26] Nakajima K, Okamura M, Kondo J N, Domen K, Tatsumi T, Hayashi S, Hara M. *Chem Mater*, 2009, 21: 186

[27] Augustine J K, Bombrun A, Sauer W H B, Vijaykumar P. *Tetrahedron Lett*, 2012, 53: 5030

[28] Sato S, Sagara K, Furuta H, Nozaki F. *J Mol Catal A*, 1996, 114: 209

[29] Shao L J, Xing G Y, He L Y, Chen J, Xie H Q, Liang X Zh, Qi Ch Z. *Appl Catal A*, 2012, 443-444: 133

[30] Darmstadt H, Roy C, Kaliaguine S, Kim T-W, Ryoo R. *Chem Mater*, 2003, 15: 3300

[31] Wang Y, Liu Y M, Li X H, Wu H H, He M Y, Wu P. *J Catal*, 2009, 266: 258

# 碳-硅复合介孔磺酸催化剂的制备及其在缩醛(酮)反应中的应用

方　林，张　坤#，陈　露，吴　鹏*
华东师范大学化学系上海市绿色化学与化工过程绿色化重点实验室, 上海200062

**摘要**: 采用浸渍法将糠醇负载在铝改性的SBA-15介孔孔道中, 经550 °C不完全碳化制备了结构规整、含多苯环的中空管状硅碳复合介孔材料. 结果表明, 通过温和磺酸化作用可使磺酸基团成功取代在多苯环上, 其酸量随着多苯环涂层厚度变化在0.38~0.84 mmol/g范围内可控调变. 相比于蔗糖作为糖源的复合固体酸, 所制碳多苯环-硅酸催化剂具有中空碳纳米管堆积的类似CMK-5介孔结构, 以及较大的反应空间、稳定的机械性能、较高的比表面和大量可以接触的质子酸中心, 因而在大分子缩醛(酮)反应中表现了良好的催化性能.

**关键词**: 固体酸; 介孔碳; 磺酸根; 缩醛(酮)反应

## 1. 前言

固体酸催化剂具有易重复使用、使用寿命长、环境污染小等优点, 因而被广泛应用于石油炼制和精细化工等领域. 金属氧化物[1,2]、杂多酸[3,4]、磺酸功能化多孔材料[5,6]和酸性离子交换树脂[7,8]等固体酸可以替代硫酸、

脂肪酸盐[9]和有机磺酸[10]等均相酸, 用于催化多种反应中, 如贝克曼重排[11,12]、烷基化[13]、酯化及水解[5,6]、酰化[14]、醚化[15]、环氧化物及烯烃的加成与醇类的脱水[16,17]、缩合反应[18,19]和加氢重整[20]等.

最近, 为使催化剂能够有效循环使用且不污染环境, 含有磺酸基团的非均相酸如离子液体[21]、磺酸修饰的有

机无机杂化材料[22,23]以及糖碳磺酸材料[24]等得到广泛研究. Xing等[25]以SBA-15为硬模板, 填充蔗糖并进行不完全炭化制得富含碳多苯环的类CMK-3介孔碳材料, 同时采用可控磺化法将磺酸基团嫁接到多苯环骨架, 使其成为一种新型介孔固体酸. 相比于Nakajima等[26]制得的糖碳磺酸较低(2 m²/g)的比表面积, CMK-3-SO₃H比表面积接近1000 m²/g, 酸量约1.0 mmol/g, 因而在液相贝克曼重排反应中表现出优异的催化活性. 然而CMK-3-SO₃H在实际应用中, 尤其是在磺化过程中, 碳骨架结构很容易因为深度碳化而坍塌. 为了提高这种材料的可操作性和稳定性, Fang等[6]调变碳多苯环在SBA-15介孔孔道中的负载量, 然后进行简单的磺化作用, 得到了兼有大比表面积和丰富酸量的碳多苯环-硅复合固体酸材料, 是催化酯化及酯交换合成生物柴油的优良催化剂.

尽管碳多苯环-硅复合固体酸材料中, 碳多苯环增加, 可提供更多苯环被磺酸基团取代, 但由于蔗糖的随机填充导致碳多苯环在SBA-15介孔孔道内无序堆积, 易造成孔道堵塞, 使得样品比表面积急剧下降, 难以体现多孔材料的反应空间优势. 因此, 如何使样品维持高的酸量, 且具有宽敞规整的反应空间成为开发此类材料的挑战之一, 另一方面, 在众多的酸催化反应中, 缩醛化反应通常用于保护羰基醛和酮类; 同时, 缩醛也是合成类固醇、药品、油漆和香水等产品对映体化合物的主要原料, 因而具有广泛的应用前景. 该反应通常在均相酸催化条件下进行具有较高的收率和选择性[27]. 然而杂多酸[21]和离子液体等非均相催化剂的酸性较弱、热稳定性较低, 因而需要在低温反应较长时间产物收率才可达到90%以上的收率[28]; 而对于酸性高反应空间小的固体酸, 如磺酸功能化的纳米硅纤维[29], 则需在150 °C高温条件下才能得到较高收率.

本文利用由糠醇制备CMK-5的方法[30], 在Al修饰的SBA-15载体上负载糠醇, 孔道内壁富集Al酸性位以及较低温度下的真空抽取, 使糠醇在不完全焙烧条件下在孔壁上热聚形成规整的碳多苯环层, 然后对其进行磺酸功能化, 最终得到碳多苯环-硅复合介孔固体酸, 并用于缩醛(酮)反应中.

## 2. 实验部分

### 2.1. 催化剂的制备

以正硅酸乙酯(TEOS, Sigma-Aldrich)为前驱体, P123三嵌段共聚物($M_w ≈ 5800$, Sigma-Aldrich)为模板剂, 在酸性水溶液中合成SBA-15[6]. 将1 g焙烧过的

SBA-15[31]浸渍于含有0.12 g AlCl₃的25 ml无水乙醇(国药集团)溶液中(投料时摩尔比Si/Al = 20), 于室温搅拌14 h, 混和物经抽滤并用无水乙醇洗涤, 在80 °C烘干, 550 °C空气中焙烧6 h, 即得Al-SBA-15 (摩尔比Si/Al = 19.2).

在1 g该铝硅材料上负载0.5~5 g糠醇(> 98.0%, 国药集团), 室温下手动搅拌直至均匀; 然后在80 °C下热聚1 h将其移至真空系统, 在80 °C下抽空1 h以去除多余糠醇液体. 最后在N₂保护下, 升至550 °C不完全炭化6 h, 得到一系列碳硅复合材料的样品SC-$x$, 其中$x$为碳化物的质量含量(%). 将SC-$x$置于密闭容器上方, 下方预放固/液比为1/20 (g/ml)的发烟硫酸(50%SO₃/H₂SO₄, 国药集团), 在80 °C静置12 h. 取出, 固体产物用80 °C以上的热水反复洗涤, 用BaCl₂(≥99.0%, 国药集团)检测滤液无SO₄²⁻; 再经干燥后得到SC-$x$-SO₃H.

SC-$x$及SC-$x$-SO₃H在固/液比为1/20 (g/ml), 15%的HF (≥40%, 国药集团)水溶液中室温搅拌过夜, 过滤, 去离子水洗涤, 烘干, 可得到纯碳材料C-$x$或C-$x$-SO₃H. 对比催化剂蔗糖-硅复合固体酸的制备方法见文献[6].

### 2.2. 催化剂的表征

X射线粉末衍射(XRD)测试在Bruke公司D8 ADVANCE型X射线粉末衍射仪上进行, Cu-$K_α$为射线源 ($λ = 0.15406$ nm). 样品的比表面积和孔径分析在Quantachrome公司Autosorb3-B型自动物理吸附仪上进行, 吸附温度为–196 °C. 吸附前, 样品在120 °C的真空条件下处理6 h. 采用日本日立公司Hitachi S-4800型冷场高分辨率发射扫描电子显微镜(SEM)对催化剂粒径和表面形貌进行分析. 红外光谱(FT-IR)在美国Nicolet公司Nexus 670型傅里叶变换红外光谱仪上测试, KBr压片. 样品先在150 °C真空脱水处理5 h, 再在110 °C吸附吡啶0.5 h; 在150 °C下脱去物理吸附吡啶后测定其FT-IR谱. 利用Mettler-Toledo公司TG/DTA 851e型热分析仪记录样品的热失重(TG)和差热曲线(DTA).

在100 ml小烧杯中加入60 ml NaCl饱和溶液, 以及待标定样品约(0.15±0.01) g, 于室温搅拌12 h, 抽滤. 以酚酞为指示剂, 用已用邻苯二甲酸氢钾标定的NaOH溶液滴定滤液, 得到样品的酸值.

### 2.3. 催化反应

醛(酮)与乙二醇的缩合反应在100 ml三颈瓶中进行, 加入0.04 mol醛(酮), 0.048 mol醇(环己酮、环戊酮、3-戊酮、乙二醇和1,4-丁二醇来自国药集团; 苯甲醛, 异戊醛和二苯甲酮来自TCI), 40 mg催化剂, 以及5 ml环己烷(≥

99.5%, 国药集团). 三颈瓶接上冷凝管和分水器, 在90 °C下加热搅拌回流1 h, 使反应产生的水与带水剂环己烷共沸蒸出, 反应结束后取样分析. 反应产物采用美国Agilent 6890/5973N型气相色谱-质谱联用(GC-MS)仪进行定性分析. 定量分析在日本岛津14-B型气相色谱仪上进行, DB-WAX毛细管柱($\phi$ 0.25 mm × 30 m).

## 3. 结果与讨论

### 3.1. 材料结构及化学性质的表征结果

表1给出了SC-$x$-SO$_3$H材料碳多苯环负载量、磺化酸量, 以及制备过程中是否受到80 °C真空抽取多余糠醇步骤的影响. 由表可见, 碳多苯环负载量可达65%; 当为51%时, 磺化酸量可达0.84 mmol/g. 若不真空抽除, 碳多苯环负载量和磺化酸量最高为52%和0.71 mmol/g, 后者与抽真空时$x$ = 44的相同. 另一方面, 糠醇过多且不抽空处理, 容易导致负载不均匀和孔道堵塞现象. 图1(a)的XRD谱表明, 该材料在焙烧、脱除硅模板之后形成了类似CMK-3实心棍状介孔结构.

图1为各样品的XRD谱. 可以看出, 继骨架后补Al以及随后糠醇的负载, 复合材料SC-$x$依然保持了二维六方孔道结构. 碳多苯环负载量的增加使得母体介孔硅的衍射峰强度逐渐减弱, 其中[100]峰宽化, 说明糠醇的过量负载可导致介孔结构畸化. 去除硅基模板后, 多苯环材料C-$x$出现类似于CMK-5的典型介孔空管结构特征衍射峰, 即[110]峰强度强于[100]峰[30]. 说明在550 °C焙烧下, 糠醇受介孔孔壁上Al酸位作用而转化的碳多苯环, 可均匀地负载于孔壁上, 形成类似于中空碳纳米管的介孔结构. 另外, 样品中碳多苯环含量越高, 其[100]峰强度越高, 说明管壁增厚, 中空管结构向实心棍状转化(见样品C-34和C-44). 经磺化反应后, 所得样品的XRD衍射峰未发生明显变化, 说明稳定的硅基结构可保护SC-$x$-SO$_3$H在磺化作用下的有序度(见图1(b)).

图2为各SC-$x$样品的氮气吸附-脱附等温线及孔径分布图, 相应的结构性质列于表2. 可以看出, 随着碳多苯环在样品中负载量的上升, 其比表面积由SBA-15的761 cm$^3$/g降至SC-34-SO$_3$H的472 cm$^3$/g, 孔径由8.1 nm变为3.6 nm, 孔体积减小了2/3, 但是SC-$x$-SO$_3$H ($x$ < 44)样品的等温线为典型的V型, 表明其存在高度有序介孔结构. SC-34-SO$_3$H样品的等温线开始出现滞后环无法闭合的现象, 归属于有机介孔聚合物的典型结构特征, 与蔗糖填充物的无序堆积状态明显不同[6]. 这进一步证明该材料中多苯环聚合物以均匀涂层的形式负载于介孔

孔壁. 同时, 滞后环由$p/p_0$ = 0.65~0.70向低比压区$p/p_0$ = 0.5移动, 说明由于多苯环聚合物的填充孔径, 尺寸逐渐减小. 另外, 由于碳多苯环的层叠产生了相当数量的微孔(占据总体积的27%), 滞后环呈现双台阶吸脱附现象. 当$x$ > 50时, 所得样品的等温线由IV型变为I型, 其中SC-51-SO$_3$H的比表面积降至318 cm$^3$/g, 微孔体积增至48%, 前者远远高于蔗糖-硅复合材料45%C/CS-SO$_3$H ($x$ = 44)的272 cm$^3$/g[6], 表明有大量介孔存在.

去除SC-34和SC-44的硅基硬模板之后, C-34和C-44呈现IV型吸附等温线, 在$p/p_0$ = 0.35出现毛细凝聚突跃, 表明其具有规整的介孔结构. 另外, 无法闭合的滞后环表明该材料以碳多苯环作为介孔孔壁, 表面性质类似于FDU-15酚醛树脂介孔聚合物[23]. 同时, 脱除氧化硅后的C-$x$样品存在叠加的双孔径分布, 显示了典型的CMK-5结构, 即中空碳管的六方密堆积形式: 右边较尖锐的分布归属于以原先介孔孔道为载体形成的多苯环纳米管管径; 左边宽泛的分布则认为是管隙, 这取决于SBA-15母体的孔壁厚度及附着上面的其它物种如Al等[30](见图2(b)). 由表2还可以看出, 样品中随着糠醇负载量的增加, 中空纳米碳管的孔壁增厚, 从而极大地促进了大分子在孔道中的传输与扩散.

图3为C-44-SO$_3$H样品的SEM照片. 由图可见, 该样品具有类似CMK-5的介孔结构: 二维纳米管六方密堆积排列, 管壁约为2 nm, 管隙分布不规整约为 < 4 nm, 并且在磺化作用后, 该材料结构依然保持完整, 显示了稳定的机械强度和物化性质.

图4(a)为引入磺酸根的SC-34和C-34的FT-IR谱. 由图可见, SC-34-SO$_3$H样品在1000~1300 cm$^{-1}$处出现的宽峰归属于Si–O的伸缩振动吸收. 脱硅后, 所得C-34-SO$_3$H相比于未经磺化作用的C-34, 在1032 cm$^{-1}$处出现一个尖锐的吸收峰, 归属于S=O的对称伸缩振动, 表明–SO$_3$H基团已成功嫁接到碳多苯环载体上. 另外, C-34-SO$_3$H样品还在约1210 cm$^{-1}$处出现了一个较明显的吸收峰, 归属于–COOH的C=O伸缩振动, 揭示了磺化作用同时也催化部分碳氢氧有机物转化为羧酸功能基团[24,26].

吡啶吸附FT-IR谱可以直接标定固体酸活性位点的种类、强度和密度[31]. 将磺化后样品在真空环境中150 °C下干燥脱水, 再降温到110 °C吸附吡啶, 为了避免吡啶的物理吸附最后需要回升到150 °C进行真空脱附处理[6]. 图4(b)为SC-$x$-SO$_3$H系列样品经吡啶吸附后的FT-IR谱. 可以看出, 在1531~1545, 1489和1445 cm$^{-1}$处

存在明显的吡啶环伸缩振动吸收峰, 分别对应于B酸位、B酸位和/或L酸位、L酸位和/或Si–OH. 随着糠醇负载量的增加, 样品在1531~1545 cm⁻¹区域吸收峰强度基本保持不变; 至51%时吸收峰强度急剧降低. 这不仅归因于酸密度增加容易生成氢键, 减弱了吡啶与B酸位的结合, 而且证明了碳多苯环管壁的增厚导致空间位阻增大(见表2), 减小了吡啶气体分子扩散至可接触酸位的可能性.

## 3.2. 催化反应性能

酸量和比表面积是影响催化剂活性的两个主要因素, 图5比较了采用糠醇和蔗糖作填充物的复合固体酸在环戊酮和乙二醇缩酮反应中的催化活性. 由图可见, 随着有机填充物的增加, 两个固体酸的比表面积均逐渐降低; 当$x < 35$, 磺酸引入量也持续增加. $x = 35$时, 蔗糖作为填充物的复合固体酸的酸值达最高为0.70 mmol/g, 而糠醇则在$x = 50$时达最高0.84 mmol/g. 然而, 后者的比表面积比前者高出近100 m²/g. 因此, 当$x = 50$时, 糠醇-硅复合固体酸催化的缩酮反应收率达到最高 (82 mol%), 而蔗糖-硅材料仅为63 mol%. 研究表明[6], 蔗糖作为填充物时, 多苯环的无序堆积容易造成SBA-15孔道堵塞, 比表面积和孔体积急剧减小, 因此磺酸根的引入量在$x = 35$时出现拐点. 然而, 糠醇则是以均匀涂层的方式负载在SBA-15孔壁上, 有助于提高多苯环负载量, 促使较多磺酸基团的取代; 焙烧后的碳多苯环-硅复合材料呈现稳定的中空纳米管状结构在磺化作用和催化反应中提供了较大的反应空间, 使可接触酸位增多, 有利于底物和/或产物在孔道中的充分扩散.

利用不同大分子醛和酮与乙二醇或者丁二醇的缩酮反应, 我们进一步考察了SC-$x$-SO₃H固体酸的催化活性, 结果列于表3, 其中SC-34-SO₃H因其可观的可接触酸活性位以及相当大的反应空间被选作目标催化剂. 由表可见, 当选用乙二醇为醇源时, 戊醛、异丁醛、苯甲醛以及环己酮的缩合反应收率均在90%以上, 显示了SC-34-SO₃H在这类底物反应中的高催化活性(实验1, 3, 5和7). 当醇源为丁二醇时, 上述各反应收率略降低了约5%左右(实验2, 4, 6和8). 而选用3-戊酮和二苯甲酮等底

物时, 反应收率也有所下降. 这是由于它们的分子相对较大, 其扩散受到孔道尺寸的限制; 另一方面, C=O官能团处于分子中间, 易受两侧支链的位阻影响, 因此反应物与磺酸酸位接触的可能性减小, 从而导致产物收率下降(实验9~12). 但是, 比较二苯甲酮与苯甲醛反应结果, 前者与乙二醇充分反应5 h后, 收率达到56% (实验5和11). 表明SC-34-SO₃H样品具有较大的反应空间, 可完全容纳苯甲醛尺寸大小的底物(实验5), 其反应收率为91%. 二苯甲酮刚性体积约为苯甲醛的2倍, 同等容积下官能团数量仅是后者的一半, 因此该催化材料对二苯甲酮与乙二醇的催化效果也非常明显. 同样, 比较二苯甲酮与乙二醇和丁二醇的反应结果发现, 后者的收率约为前者的一半(实验11和12), 这是因为丁二醇体积比乙二醇大一倍, 能够到达酸位与二苯甲酮反应的数量也减少一半. 结果表明, 拥有数量可观的可触及酸位的SC-34-SO₃H固体酸在大分子缩酮反应中表现出较高且稳定的催化活性.

反应结束后, 过滤SC-34-SO₃H固体酸催化剂, 用过量环己烷多次充分洗涤并干燥, 用于环己酮和乙二醇的缩酮反应中考察其重复使用性能. 结果表明, 重复使用6次后, 反应收率减少了约5%. 这说明SBA-15孔道内壁富集的Al酸性位以及较低温度下的真空抽取, 使糠醇形成的碳多苯环层牢固地附着在壁上, 因而表现出较高的稳定性.

## 4. 结论

SBA-15负载的糠醇在550 °C下不完全焙烧, 可制得规整的中空管状碳多苯环-硅介孔复合物, 该复合物经过磺酸作用, 酸量最高可达0.84 mmol/g. 相比于蔗糖作为糖源的复合固体酸, 所制碳多苯环-硅酸催化剂具有中空碳纳米管堆积的类似CMK-5介孔结构、较大的反应空间、稳定的机械性能、较高的比表面积以及大量可以接触的B酸位, 因而在大分子缩醛(酮)反应中表现出很高的催化性能, 且制备方法简单易于重复使用, 有望在实际的酸催化反应得到广泛应用.